EUROPEAN ORGANIZATION FOR NUCLEAR RESEARCH

CERN/ISRC/74-3
9 January 1974

INTERSECTING STORAGE RINGS COMMITTEE

A PROPOSAL TO UPGRADE THE ELASTIC SCATTERING SET UP IN I6 FOR A FURTHER INVESTIGATION ON THE ELASTIC SCATTERING AT LARGE ANGLES, DIFFRACTION DISSOCIATION AND THE SEARCH FOR SOME NON-DIFFRACTIVE QUASI-TWO BODY PROCESSES

L. Baum, M. Block, G. DeZorzi, R. Ellis, R. Glauber, B. Gobbi, H. Hilscher, J. Layter, A. Lecourtois, F. Lobkowicz, A. Kernan, D. Miller, F. Muller, B. Naroska, C. Rubbia, G. Sette, D. Schinzel, A. Staude, J. Tarnopolski and G. Trilling

CERN, Geneva, Switzerland

Department of Physics, Harvard University, Cambridge, Mass., USA

Istituto di Fisica dell'Università and INFN, Sezione di Genova, Genova, Italy

Sektion Physik der Universität, Munich, Germany

Northwestern University, Evanston, Ill., USA

University of California in Riverside, Riverside, Calif., USA

1. INTRODUCTION

We would like to introduce significant hardware improvements to the set-up for the study of the large angle elastic scattering at the ISR. Adding to the detection capability of our former detector makes it possible to study simultaneously both the large angle scattering with an increased $|t|$ resolution and about thirty times the old event rate and, in addition, a number of very interesting new processes. We believe that at least six to eight months of data taking are necessary in order to complete these investigations. Our interest beyond this time is oriented toward the experimental program described in the document ISRC/72-32 Add. 3. The bulk of the new detection equipment is a necessary part of the subsequent experiment. If approved, the present experiment would provide not only a large amount of important physics information but also an extremely valuable "field" experience of such novel devices, almost inevitable before constructing a detector of the size of the one proposed in the document ISRC/72-32 Add. 3.

Our main physics objectives can be subdivided into three topics:

i) Elastic scattering at large $|t|$, $p + p \to p + p$, with special consideration of the region of the minimum found in our previous investigations and at $|t| > 5$ GeV^2 which is so far a totally unexplored region.

ii) Diffractive dissociation, $p + p \to p + X$. Low mass (< 3 GeV/c^2), low multiplicity X objects can be fully reconstructed; X objects of larger masses can be identified by missing mass. In this case we can measure rapidity and multiplicity distributions of the decay of the object X. The reaction can be observed over a $|t|$ range from 0.1-0.2 GeV^2 to the largest values permitted by the rate.

iii) Search for charge exchange processes of the type $p + p \to (\pi^+ + p) + (\pi^- + p)$ or $p + p \to n + (\pi^+ p)$. The cross-sections for these non-diffractive processes, typically a fraction of a millibarn at PS energies, at least according to the simplest Regge phenomenology, are expected to drop like $1/s^{\alpha}$, with $\alpha = 2$ for π-exchange dominance, and $\sqrt{s}$ the centre-of-mass energy. The observation of the residual amplitude at very high energies would give information on the validity of the Regge description in a totally unexplored region.

All three measurements are to be performed with the same set-up and slightly different trigger requirements according to three different priority levels of data recording.

The hardware additions to the set-up (Fig. 1) are motivated initially by the requirements of the measurements on the large angle elastic scattering and the intention of retaining a certain amount of compatibility with the experiment R603 in the eventuality that more running time is allocated to this experiment by the ISRC. The main consequence of this last assumption is that the spectrometer magnet should remain in a R603 compatible configuration, rather than the one of the experiment R602, since a conversion of the magnet would require a few months of interruption at each change-over. Therefore we must add some chambers and an energy measuring device in the arm opposite to the spectrometer (arm 2). Ideally one would like an additional spectrometer magnet, unfortunately much too expensive and too long to construct. Another perfectly acceptable and much simpler solution consists of replacing the magnet with a total absorption calorimeter preceded by a few planes of chambers (see Appendix I). The energy resolution of this device is 5-10% at 24 GeV and this is adequate, for instance, in identifying elastic scattering events to the largest angles. Another interesting advantage of the calorimeter is that no computing is required to extract the energy information and this condition can be used to set up an efficient elastic scattering trigger at large $|t|$. The calorimeter is also essential for the study of the non-diffractive process.

The second addition consists of planes of drift chambers with two-dimensional read-out, which are introduced in each of the eight proportional chamber supermodules of the spectrometer magnet of arm 1. In this way we can improve by $\sim$ 10 times the momentum resolution of the high-energy particles and at the same time resolve the problem of sorting ambiguities in multitrack events. This is completely trivial then since the read-out is giving directly pairs of coordinates in space.

The timetable for the construction of the two additions is unusually short since, according to the recommendations of the ISRC on our proposal 72-32 Add. 3, we have pursued for some time a very active programme of technical developments on drift chambers and total absorption calorimeters. One of the two calorimeters required is half constructed and we expect

to complete the construction of both units by June 74. The development work on drift chambers is completed and we are ready to construct the final detectors. We can be ready at the end of the small-angle elastic scattering experiment provided the response of the ISRC is not too long delayed.

2. THE LARGE-ANGLE ELASTIC SCATTERING

The information available today on the large-angle elastic scattering at ISR energies is rather incomplete. This is clearly demonstrated in Fig. 2, where we display the totality of the available data. Crucial questions, like the general s-dependence of the process are still largely unknown. An interesting region is the one around the observed minimum. We would like to extend the observation of the effect at all available ISR energies and to make a precision determination of its shape and of its position. The experimental resolution of the first experiment was comparable to the width of the dip, and its true shape is still unknown. In general, a systematic precision study of the process at all angles is of considerable importance and far from being completed.

The kinematics of the elastic process is shown in Fig. 3, where the scattering angle is plotted as a function of the beam momenta and for a constant value of the four-momentum transfer $|t|$. For values $|t| > 7$ GeV^2 we do not expect to be able to perform observations, at least at present ISR luminosities. If we are interested in observing the elastic process from $|t| > 0.5$ GeV^2 to the largest values possible and over the whole ISR range (11 to 31 GeV), the detector must be sensitive from 20 mrad to approximately 200 mrad at 11 + 11 GeV. A maximum angle of 160 mrad is still quite acceptable for the higher energies and for the lower energies it is unlikely that the ISR could provide anything close to its maximum luminosity.

The specified angular range can be satisfied without difficulty in arm 2, where the calorimeters can be located easily to the correct angles. More elaborate is the problem of arm 1, where the spectrometer was originally designed for a maximum angle of 100 mrad. Some increase of the maximum angle could be achieved by approaching the magnet to the interaction point. We intend to increase further the angle of acceptance by widening the magnet gap from 64.5 cm to 100 cm, introducing two iron spacers in the return yokes.

Finally we can also retain events in which the proton track hits the pole pieces in the second half of the magnet. In this way we can achieve the required maximum angle of 160 mrad and to extend it to $\sim$ 200 mrad at the expense of some loss in the momentum resolution. This loss appears acceptable, since this angular extension is necessary only at the lowest ISR energies where the sagitta is comparatively large and the collinearity requirement most effective. Finally, we can tighten the anticoincidence shield all around the interaction point and in this way reject part of the inelastic events. It is evident that if possible, running with asymmetric energies and the higher momentum in beam 1 would also extend the acceptance of the detector to large angles.

It is important to remark that the region around the minimum occurs at $|t| \simeq 1.2$ GeV^2 and it is well within the acceptance for all ISR energies.

High rate and excellent momentum and angular resolutions are crucial for a good observation of the elastic process at large angles. An excellent angular resolution is also required in order to determine with precision the value of $|t|$. The present magnetic spectrometer has a rather coarse momentum resolution because of the relatively wide wire spacing of the proportional chambers (2 mm). For instance the momentum resolution at 26 GeV is now of the order of 25% FWHM. In order to overcome the rather limited spatial resolution of the proportional chambers we intend to add to each supermodule a set of drift chambers with a spatial resolution of the order of 0.1-0.2 mm in the plane relevant to the magnetic deflection. With this addition the errors in the spatial reconstruction become comparable to the contributions of the Coulomb multiple scattering and to the initial spreads of the circulating beams (see Appendix II).

The data rate of the new experiment is considerably improved with respect to the older one:

i) A factor of 2.5 is due to the increased azimuthal acceptance.

ii) A factor of the order of 3-4 is gained, since now we have proportional chambers with no appreciable recovery time and we can set up a much more restrictive trigger based on the information of the calorimeters.

iii) A factor of at least 3, since the average ISR luminosity has considerably increased with respect to the times in which the bulk of the data were collected for the first time.

Finally a few remarks on data reduction. A very efficient selection of the events can be made by simple requirements of absence of other charged or neutral tracks in addition to the two protons, an energy requirement in the calorimeter(s), and a collinearity of tracks. Note that the probability of spurious tracks is negligible because of the excellent resolving time of the proportional chambers. Only relatively few clean events require tracking through the rather homogeneous field of our magnet. In the older experiment this last operation required about 200 μsec on the 7600. Even adding the computing required for event-sorting, histogram-filling, and the Monte Carlo for the corrections in the detection efficiency, the computer requirements remain relatively modest, mainly because of the simplicity of the topology of the events.

3. DIFFRACTION DISSOCIATION $p + p \rightarrow p + X$

The trigger requirement of the last large-angle scattering experiment almost accidentally selected also a large number of diffraction dissociated events. This is shown in Fig. 4, where one notices a very remarkable enhancement of the diffractive bands associated with the low multiplicity requirements. Some results from these data have been reported. The upgraded detector offers the possibility of greatly extending the investigations on the process.

The process of diffraction dissociation at ISR energies appears to be of considerable theoretical interest because of its relatively large cross-section and its specific features. From the experimental point of view the kinematics is easier to reconstruct than in the case of the general "double jet" event. In a way, this is the next natural step after the elastic scattering process. As yet, in spite of its fundamental nature, very little is known on the process at high energies.

We would like to study the process $p + p \rightarrow p + X$ in two different configurations. In the first configuration the single proton is analysed by the spectrometer magnet and the decay of the X object is observed with the chambers of the telescope of arm 2. This configuration is most suited for missing-mass determination and the observation of global decay properties of X, like multiplicities, rapidity distributions, etc. The second configuration of interest is the one in which the single proton is detected by the calorimeter and the X object decays inside the acceptance of the

spectrometer magnet. It is very likely that only low mass and low multiplicity objects can be studied in this way, although it is likely that some sort of information could be extracted also for the events which miss partially the acceptance of the spectrometer.

The basic kinematics for a missing-mass experiment are shown in Fig. 5. Missing-mass experiments are possible only for relatively large values of the mass of the X object (given by the approximate formula $m_X^2 = s(1 - x)$ where x is the standard Feynman variable for the recoiling proton) since the resolution in the missing mass (Fig. 6) is largely insufficient at lower masses. We have assumed an over-all momentum resolution of the order of 1%, which is a realistic value of the combined errors in the momentum spread of the circulating beams and of the momentum analysis of the scattered particle. Of course the distribution of the missing mass could be of considerable interest if indeed there is an appreciable production of heavy objects, as suggested for instance by our earlier observations. If large mass objects exist, we can measure the topology of the decay with the drift chambers of arm 2. Evidently if such objects were produced with a significant cross-section, the study of their decay properties would be in itself a very extensive field of study.

The missing-mass technique can be replaced for lower masses with a determination of the effective mass of the decay products of the X object. The detection efficiency of the spectrometer has been evaluated for a number of three-body decays and found acceptably large for masses below approximately 3 GeV/c^2. Although the detection efficiency is going to be without doubt a fundamental limitation of this method, the mass resolution is typically a few MeV and the existence of structure in the mass spectrum can be very carefully investigated as a function of the four-momentum transfer $|t|$ and of the centre-of-mass energy $\sqrt{s}$. It is of considerable interest to see which of the N^* states are produced, if any.

The trigger requirement for diffractive events is particularly simple and it consists of one and only one track in one arm and a multiparticle event in the other. In addition a sizeable amount of energy must be deposited in the calorimeters. Since the cross-section for diffractive processes is relatively large we expect that the trigger rate could be as large as a few kilocycles during the high luminosity runs. The data

acquisition system saturates at approximately 200/sec. The diffractive trigger would then have the lowest relative priority and fill up the unused fraction of the acquisition time.

The off-line data processing is the main limitiation to the quantity of data we can collect with this type of trigger. On the basis of past experience we estimate that we can process on the 7600 of the order of 100 events/sec. A previous filtering using our on-line facility should reduce the volume of data by at least a factor of 10 with simple topology requirements. Therefore about 200 equivalent hours at the 7600 should be adequate to process of the order of 1000 hours of data taking. We remark that this corresponds to about 3×10^8 raw triggers and 10^6-10^7 diffraction events of different types.

4. SEARCH FOR CHARGE-EXCHANGE PROCESSES

M. Block and some of us had proposed some time ago an investigation on a number of quasi-two-body decays of resonances produced in pp collisions. The experimental apparatus is very close to the one we propose in this document. We have been approached by the above group about the possibility of performing this experiment in parallel with the study of the elastic scattering at large angles and of the diffraction dissociation.

More specifically the physics proposed is the study of the quasi-two-body reactions:

$$pp \to \Delta^{++}\Delta^{0} \qquad (1)$$

$$pp \to \Delta^{++}n \qquad (2)$$

$$pp \to \Delta^{+}\Delta^{+} \qquad (3)$$

$$pp \to \Delta^{+}p \qquad (4)$$

The first two charge-exchange reactions study $\rho + A_2$ exchange, which at the upper end of the ISR energy domain should dominate over pion exchange. Reaction (3) and (4) may have dominant Coulomb contributions. For details we refer to the documents ISRC/73-21 and ISRC/73-21 Add. 1. Here we would like to point out that (i) we are interested in extending our work to the above-mentioned channels in collaboration with the Northwestern group, and (ii) that the data taking for these channels can be performed essentially in parallel with the other two processes.

APPENDIX I

THE DETECTOR IN ARM 2

The design parameters and the constructional details of the fine grain calorimeters have been described to the ISRC in the previous note (ISRC/72-32 Add. 4) to which we refer for detail. We would like to position the two steel plate calorimeters one above and the other below the beam line (Fig. 1). The planes of chambers, in front of the calorimeter, approximately 1 m apart, are used to localize the charged particles. A hodoscope, approximately 1 interaction length inside the calorimeter is used to determine the position of the hadronic jets. Chambers and calorimeters rigidly fixed to one another can be moved on rails along the beam line, in order to adjust the maximum and minimum angles of detection according to the momentum of beam 2. The smallest angle of detection is $\sim$ 10 mrad and the largest 200 mrad.

Since the efficiency of light yield of the calorimeter is some 30% greater for electromagnetic than for nuclear cascades, the first element of the calorimeter is a 15 radiation length γ-ray converter consisting of a sandwich of 3 mm thick lead plates and 3 mm liquid scintillator gaps. The γ-counters have already been described in detail in the document ISRC/73-32 Add.3 to which we refer.

Both the γ-detector and the calorimeters are also parts of the set-up proposed in the above-mentioned document ISRC/73-12 Add. 3.

The list of the main parameters of the calorimeter is given in Table 1.

APPENDIX II

THE UPGRADING OF THE MAGNETIC SPECTROMETER

The magnetic spectrometer is already equipped with four sets of proportional chambers, two before and two after the magnetic field volume. Shortly, a fifth set of planes, the magnet chambers, will be added at the centre of the magnetic volume. Each set of planes (supermodule) consists of an X,Y pair with 2 mm wire spacing, oriented parallel and perpendicular to the average magnetic field direction and of a U,V pair of planes with spacing of $2\sqrt{2}$ = 2.828 mm, with wires orthogonal to each other and at ± 45° with respect to the X,Y pair. The purpose of the cross wire orientations is to remove ambiguities in the pairing of tracks between views. In order to allow for some inefficiency of the wire planes the pattern recognition program requires only a triplet of planes in order to define a valid hit. In the case of several hits occurring simultaneously the sorting procedure is very laborious, computer-time-consuming and very often ambiguous. In this case all possible solutions must be retained up to the track finding and eventually through the tracking in the magnetic field. Ghosts can be eliminated in certain cases by more restrictive geometrical and kinematical constraints. In practice this procedure is highly sensitive to the presence of additional spurious tracks of γ-rays converting the vacuum chamber or elsewhere.

Another unsatisfactory feature of the present magnetic spectrometer is its relatively coarse momentum resolution, mainly due to the short lever arm available within the interaction region and the wide wire spacing of the proportional chambers (2 mm). Adding the fifth supermodule inside the magnet is expected to improve the momentum resolution somewhat, but not enough to match the limiting value of 0.6% due to the multiple Coulomb scattering and the "natural" momentum spread of the ISR stacks of 1% (Fig. 7). A good momentum resolution for particles of momentum close to the one of the circulating beams is crucial for the observation of the elastic scattering and of the diffraction dissociation.

We propose to resolve at the same time the problem of the pattern recognition and of the insufficient momentum resolution by completing

each of the supermodules with a simple drift chamber unit with wires parallel to the magnetic field direction, and a two-dimensional read-out. On the basis of our recent tests we would like to construct wire chamber planes with the structure shown in Fig. 8. The basic drift cell is 5 cm wide and 1 cm thick and it has a single sense wire of 50 μ diameter. A set of cathode wires at four different negative potentials generate the electrostatic field configuration in the cell. The field is such that the electric field at all distances from the sense wire is strong enough to saturate the drift velocity of the electrons. Close to the sense wire there are two cathode electrodes made of very thin photoetched delay lines with a longitudinal propagation speed 10^{-2} of the speed of light (Fig. 9). Avalanches occurring along the sense wire induce electrostatic charge images onto the delay line, which propagate to both ends with the characteristic transmission speed. In practice we can collect 20% of the charge induced onto the main wire. This is sufficient for a precise determination of the times of arrival t_1, t_2 of the leading edges of the pulses at both ends of the line. The longitudinal position of the avalanche is linearly related to the time difference $t_1 - t_2$. Results of our tests give a precision of this coordinate which is better than 1/100 of the total length of the wire. The drift time t_0 between the passage of the particle and the arrival of the first electron avalanche provides a determination of the other coordinate perpendicular to the wire to perhaps 100 μ r.m.s. deviation. In order to remove the left-right ambiguities and to correct for the time of drift of the electrons, we compose a stack with two such drift planes off-set, with respect to each other, by one half of the spacing between the sense wires. A list of the main parameters of the spectrometer is given in Table 2.

A non-trivial part of the device is the read-out electronics to measure the time of drift and the delay of collection of the image charges. Our basis for the time measurement is the so-called "time stretcher" which expands the time elapsed by approximately thirty times, such that it can be measured with slow and relatively inexpensive TTL scalers. The cost of the electronics is of the order of 100 Sw. Fr. per channel.

Table 1

List of parameters of the calorimeter

Calorimeter	
Number of modules	24
Number of steel plates/module	26
Number of scintillation gaps/module	25
Number of PM/module	2
Scintillator	NE235
Gap width of scintillator	3 mm
Thickness of steel plate	3 mm
Total weight/module	$\sim$ 800 kg
Dimensions	
i) vertical	85 cm
ii) horizontal	125 cm
iii) thickness of 1 module	15.6 cm
Angle acceptance (with chambers)	
i) minimum angle	$\sim$ 10 mrad
ii) maximum angle	200 mrad

Table 2

List of parameters of the magnetic spectrometer

Magnet	
Magnetic field	0.5 T
Apertures	
i) vertically	100 cm
ii) horizontally	80 cm
Max. angle acceptance with magnet centre at 5 m	
i) particles to last chamber	150 mrad
ii) particles to middle chamber	200 mrad
Min. angle acceptance	
i) magnet	12 mrad
ii) magnet and chambers	16 mrad
Detectors	
Number of prop. chambers	40
Total number of wires	12000
Number of drift chambers	10
Number of drift chamber wires	$\sim$ 280
Expected momentum resolution at 26 GeV	
i) proportional chambers	5.5% s.d.
ii) with addition of drift chambers	$\sim$ 1.0% s.d.

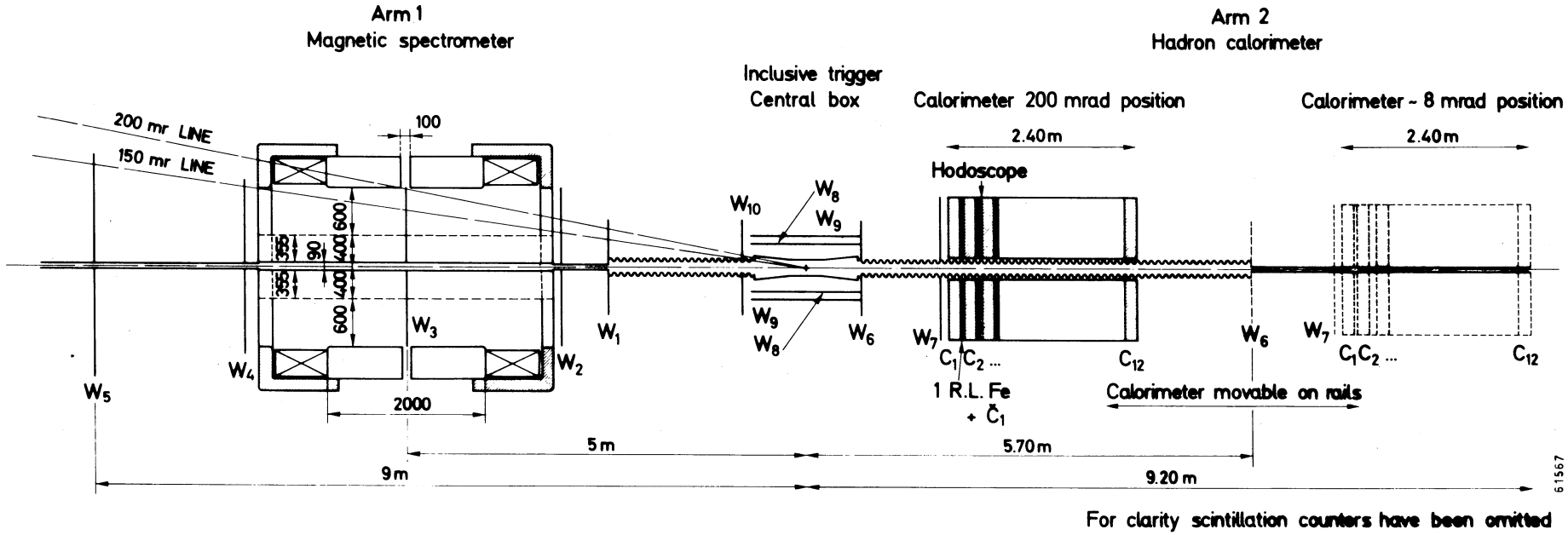
Arm 1
Magnetic spectrometer
Inclusive trigger
Central box
Arm 2
Hadron calorimeter
Calorimeter 200 mrad position
Calorimeter - 8 mrad position
200 mr LINE
150 mr LINE
100
2.40m
2.40m
Hodoscope
W10
W8
W9
W9
W8
W6
W7
W6
W7
W5
W4
W3
W1
W2
C1 C2 ...
C12
C1 C2 ...
C12
1 R.L. Fe
+ C1
Calorimeter movable on rails
600
400
90
400
600
355
355
2000
5m
5.70m
9m
9.20 m
61567
For clarity scintillation counters have been omitted

Fig. 1

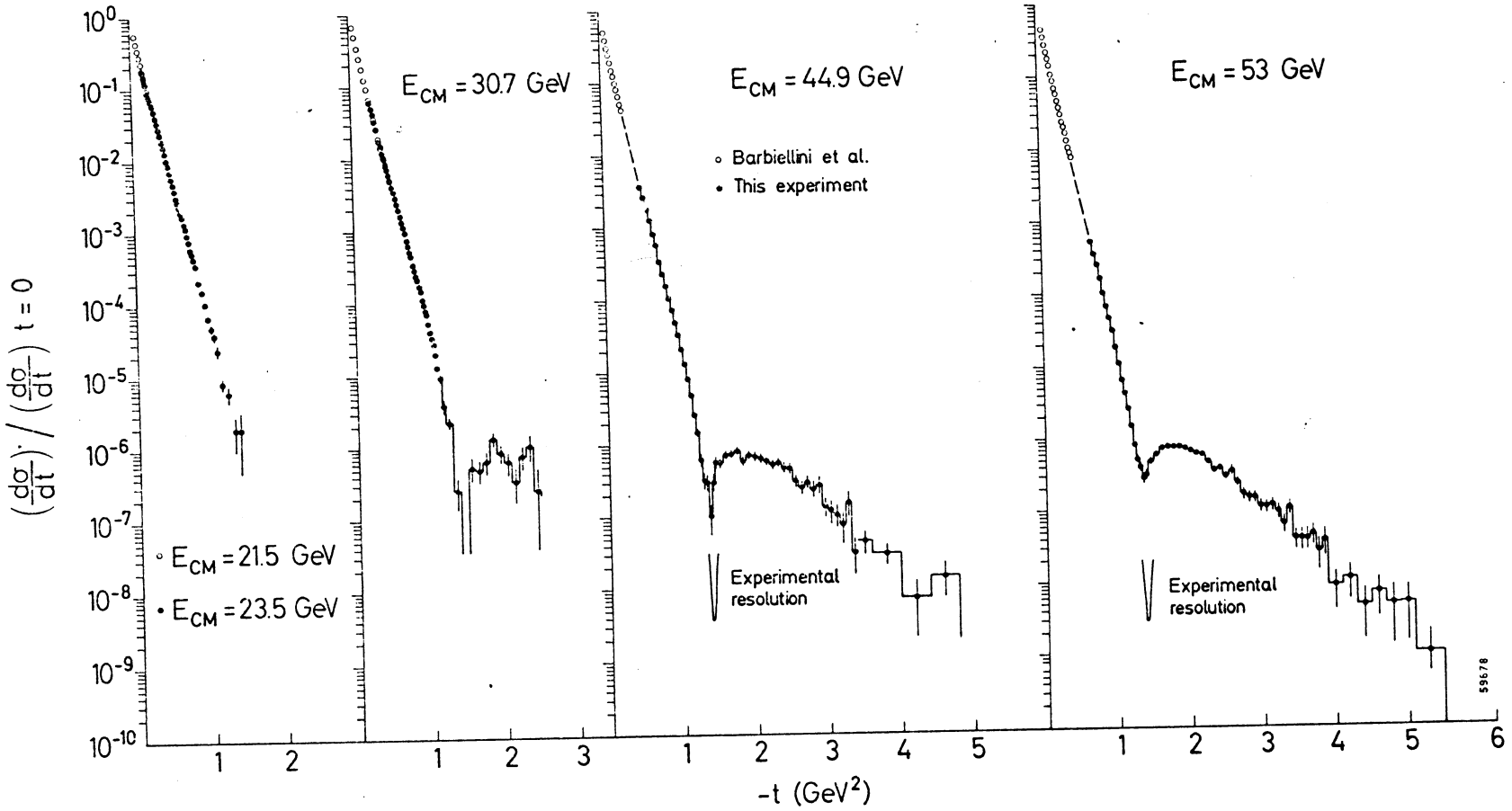
E_{CM} = 30.7 GeV
E_{CM} = 44.9 GeV
E_{CM} = 53 GeV
Barbiellini et al.
This experiment
E_{CM} = 21.5 GeV
E_{CM} = 23.5 GeV
Experimental resolution
Experimental resolution
$\left(\frac{d\sigma}{dt}\right) / \left(\frac{d\sigma}{dt}\right)_{t=0}$
$-t\ (GeV^2)$
596 78

FIG. 2

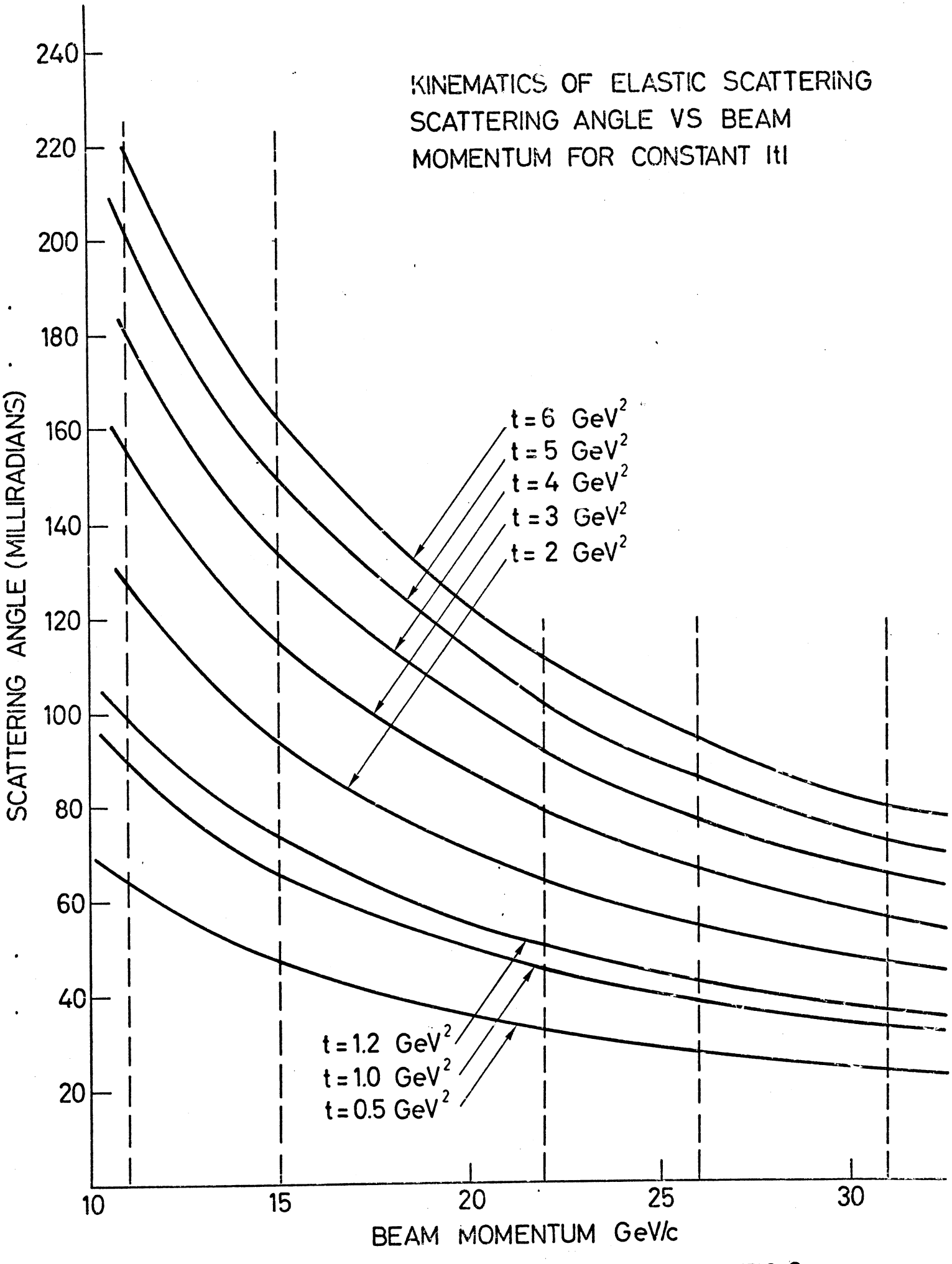
KINEMATICS OF ELASTIC SCATTERING
SCATTERING ANGLE VS BEAM
MOMENTUM FOR CONSTANT |t|
SCATTERING ANGLE (MILLIRADIANS)
240
220
200
180
160
140
120
100
80
60
40
20
t = 6 GeV²
t = 5 GeV²
t = 4 GeV²
t = 3 GeV²
t = 2 GeV²
t = 1.2 GeV²
t = 1.0 GeV²
t = 0.5 GeV²
10
15
20
25
30
BEAM MOMENTUM GeV/c

FIG.3

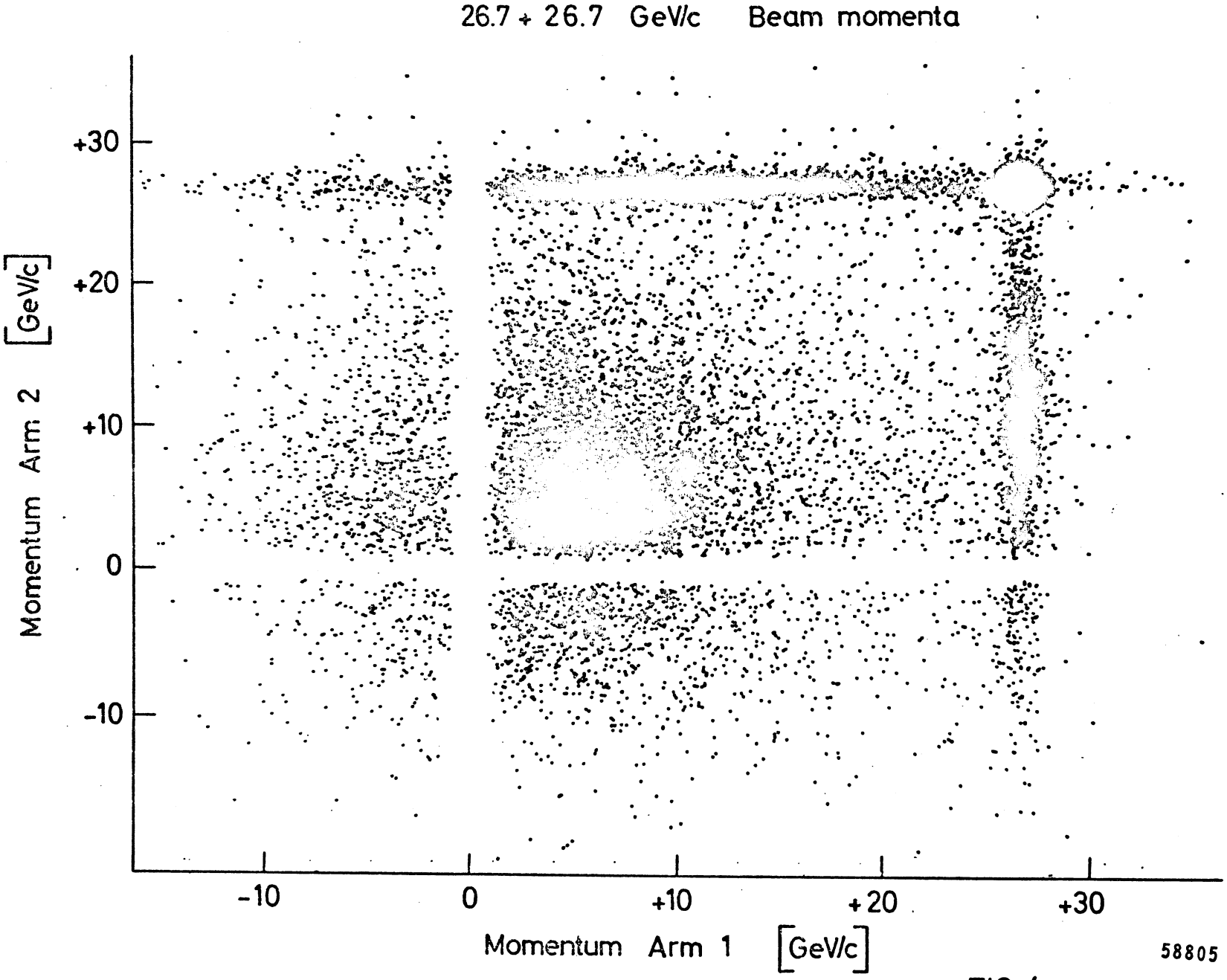
26.7 + 26.7 GeV/c Beam momenta
+30
+20
+10
0
-10
Momentum Arm 2 [GeV/c]
-10
0
+10
+20
+30
Momentum Arm 1 [GeV/c]
58805

FIG. 4

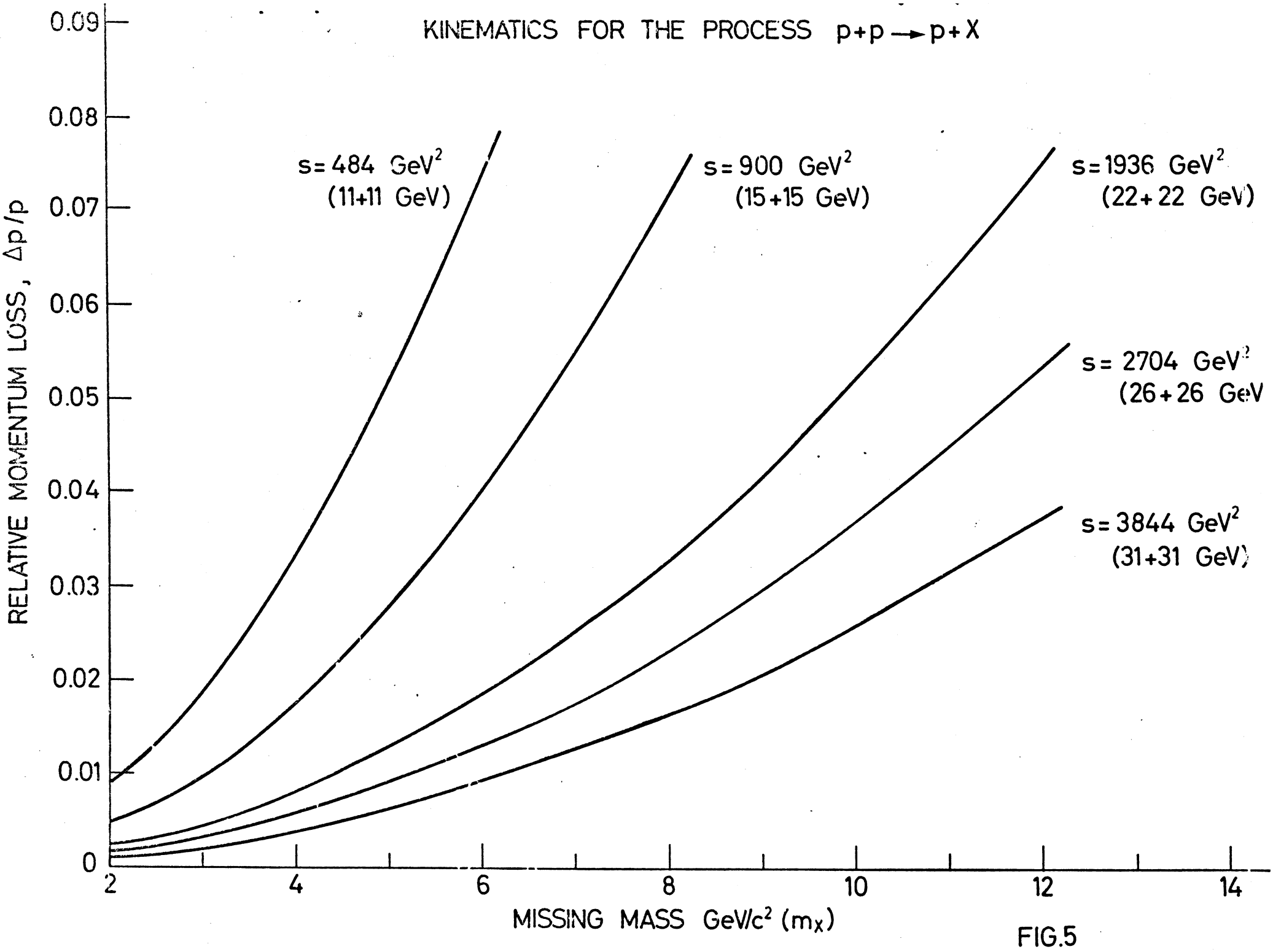
KINEMATICS FOR THE PROCESS p+p → p+X
RELATIVE MOMENTUM LOSS, Δp/p
0.09
0.08
0.07
0.06
0.05
0.04
0.03
0.02
0.01
0
s = 484 GeV²
(11+11 GeV)
s = 900 GeV²
(15+15 GeV)
s = 1936 GeV²
(22+22 GeV)
s = 2704 GeV²
(26+26 GeV
s = 3844 GeV²
(31+31 GeV)
2
4
6
8
10
12
14
MISSING MASS GeV/c² (mx)

FIG.5

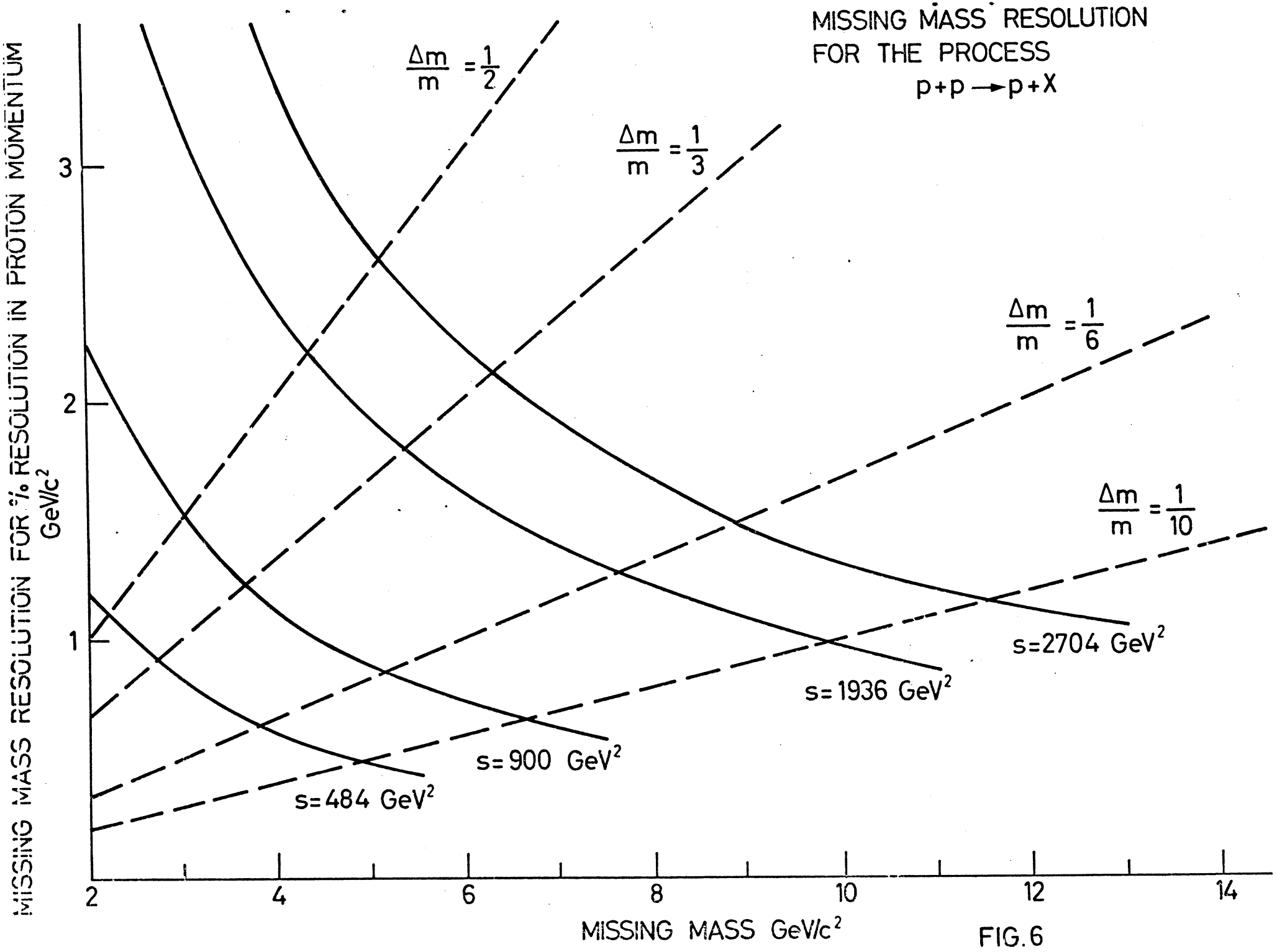
MISSING MASS RESOLUTION
FOR THE PROCESS
p+p → p+X
Δm/m = 1/2
Δm/m = 1/3
Δm/m = 1/6
Δm/m = 1/10
s=2704 GeV²
s=1936 GeV²
s=900 GeV²
s=484 GeV²
MISSING MASS RESOLUTION FOR % RESOLUTION IN PROTON MOMENTUM GeV/c²
MISSING MASS GeV/c²
1
2
3
4
6
8
10
12
14

FIG.6

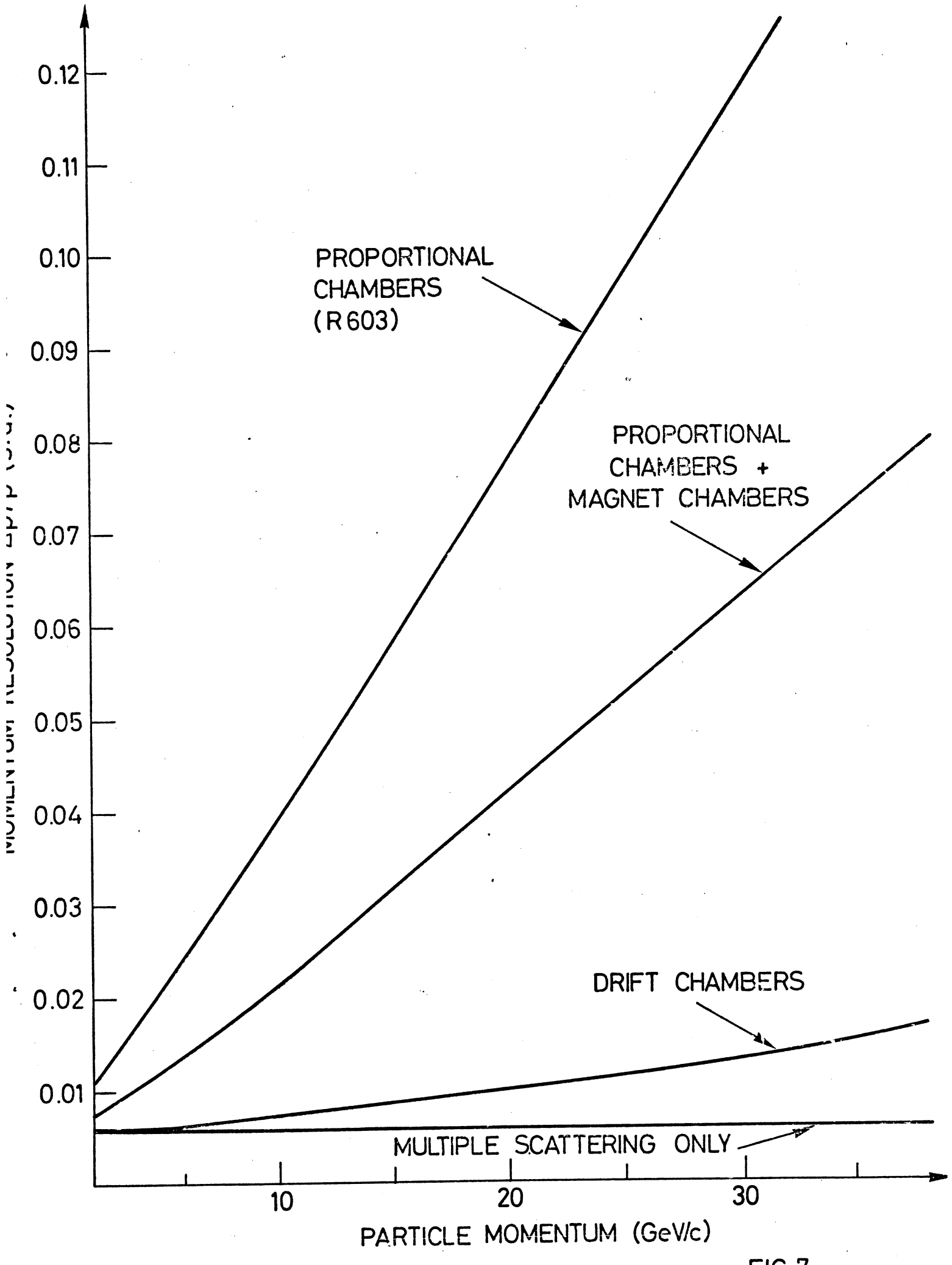
0.12
0.11
0.10
0.09
0.08
0.07
0.06
0.05
0.04
0.03
0.02
0.01
PROPORTIONAL
CHAMBERS
(R603)
PROPORTIONAL
CHAMBERS +
MAGNET CHAMBERS
DRIFT CHAMBERS
MULTIPLE SCATTERING ONLY
10
20
30
PARTICLE MOMENTUM (GeV/c)

FIG.7

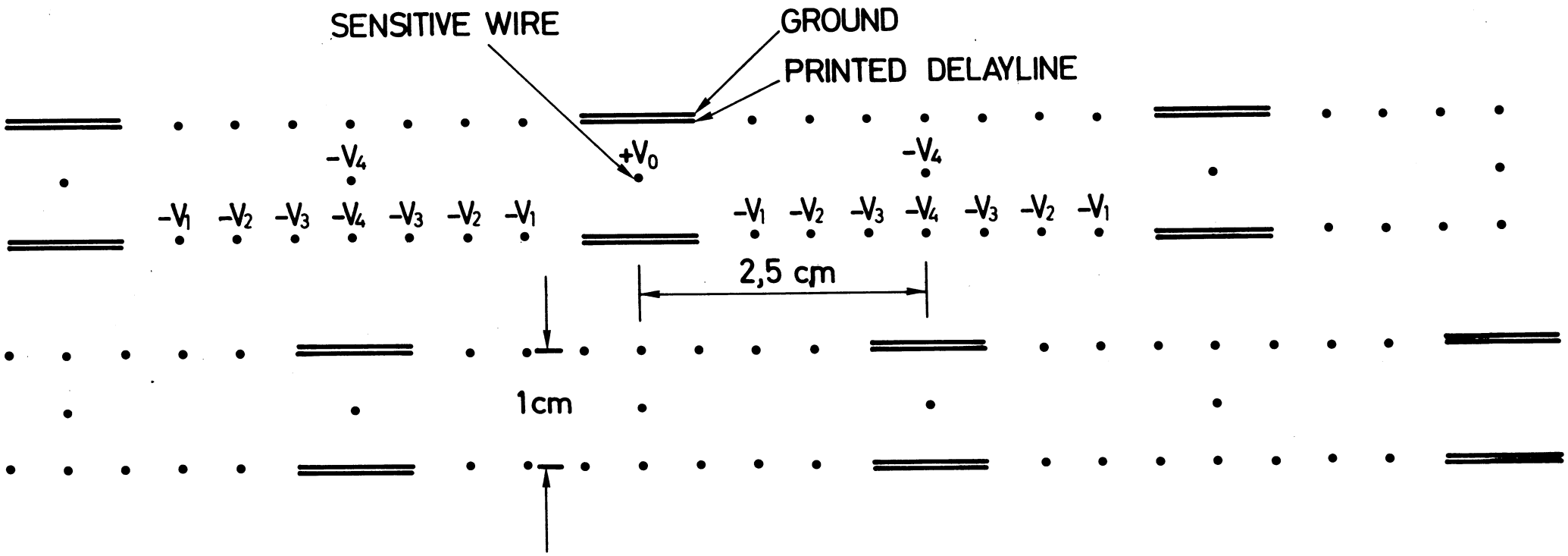
SENSITIVE WIRE
GROUND
PRINTED DELAYLINE
-V4
+V0
-V4
-V1 -V2 -V3 -V4 -V3 -V2 -V1
-V1 -V2 -V3 -V4 -V3 -V2 -V1
2,5 cm
1cm

FIG. 8

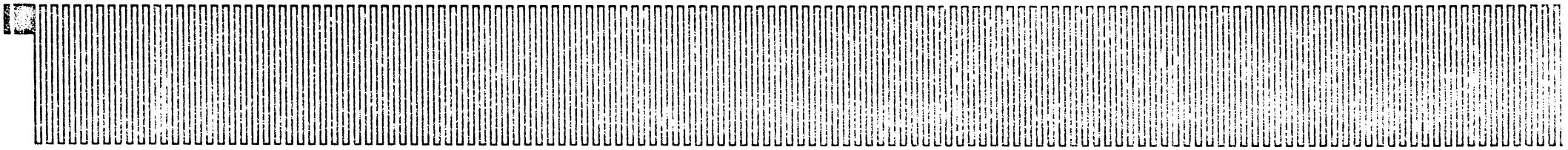

FIG. 9